Available at
http://pvamu.edu/aam
Appl. Appl. Math.
ISSN: 1932-9466

Applications and Applied Mathematics:
An International Journal
(AAM)

Vol. 13, Issue 1 (June 2018), pp. 516 - 534

Study of Soret and Ion slip effects on MHD flow near an Oscillating Vertical Plate in a Rotating System

U.S. Rajput and Mohammad Shareef

Department of Mathematics and Astronomy
University of Lucknow
Lucknow-226007, India
E-mail: rajputshareeflu@gmail.com

Received: June 30, 2017; Accepted: April 28, 2018

Abstract

This study analyses the Soret, Hall and ion slip effects on a free convective flow of an electrically conducting, incompressible and viscous fluid near the vertical oscillatory infinite plate in a rotating system. A set of dimensionless governing equations of the model is obtained. As the equations are linear, an exact solution can be obtained by using Laplace transform method. The influence of various parameters on the concentration, temperature, velocity, Sherwood number and Nusselt number are discussed with the help of graphs. The numerical values of skin-friction are shown in tables. Applications of the study arise in field like planetary and solar plasma fluid dynamical systems, magnetic field controlled materials processing systems, rotating MHD induction machine energy generators etc.

Keywords: MHD, Rotating fluids, Porous medium, Thermal convection

MSC 2010 No.: 76W05, 76U05, 76S05, 76E06

1. Introduction

The flow of electrically conducting fluid under the influence of magnetic field has a great significance in science and engineering. Therefore, many researchers like Soundalkar (1979), Prasad et al. (2007), Ganesan and Laganathan (2002), Raptis (1998), Muthucumaraswamy et al. (2001) and Hossain & Takhar (1996) have worked in this field. When the strength of the magnetic field is small or moderate, then the Ohm's law can be used by ignoring the ion slip and Hall term. Cowling (1957) emphasized that if the applied magnetic field is large enough, these terms need to be considered with Ohm's law.

The production of an additional potential difference transverse to the direction of drifting free charge and applied magnetic field (perpendicular to the flow of charge) between the opposite surfaces induces an electric current perpendicular to both the fields, magnetic and electric. This current is known as Hall current. The phenomenon is termed as Hall Effect. The first practical application of Hall Effect was in the 1950s as a microwave power sensor. Nowadays, there are many products that include Hall Effect devices, ranging from machine tools to medical equipments, automobiles to aircrafts, computers to sewing machines, and in the field of energy such as Hall accelerators and MHD generators etc. Due to their wide applications, many types of researches have been carried out by taking models of MHD flow with Hall current. Some of them are mentioned in the next paragraph.

Watanabe and Pop (1995) analyzed the effect of Hall current on magneto-hydrodynamic boundary layer flow over a continuous moving plate. Hall current effect on free convective magneto-hydrodynamic flow past a semi-infinite vertical flat plate with the mass transfer was studied by Abo-Eldahab and Elbarbary (2001). Further, Jaimala et al. (2013) analyzed the effect of magnetic field and Hall current on an electrically conducting couple-stress fluid layer heated from below. It was concluded by them that in the presence or absence of Hall current, magnetic field has a stabilizing effect on the thermal convection. Rajput and Gaurav (2016) examined the unsteady MHD flow in the presence of Hall current with variable temperature and mass diffusion along impulsively started inclined plate. Further, Mazumdar et al. (1976) presented the steady MHD flow with the Hall Effect. The combined effect of Hall current and dissipation on free convective MHD flow in a rotating system was analyzed by Agarwal et al (1983). They found that the primary shear stress increases and secondary shear stress decreases with increase in magnetic and Hall parameters. Effect of Hall current with ion-slip on Couette flow with heat transfer was studied by Attia (2005). Further, he (2009) extended his own work by taking exponentially decaying pressure gradient.

Also, the rotating fluids have their abundant geophysical and astrophysical applications. Some natural phenomena such as tornadoes, geophysical systems, ocean circulations, hurricanes etc, imply rotating flows with heat and mass transfer. Several articles and books on heat transfer and hydrodynamic characteristics of rotating flows have been published: Greenspan (1968), Soong and Ma (1995), Owen and Rogers (1989), Muthucumaraswamy et al (2013), Soong (2001) etc. Further, in the fluid flow problems with heat and mass transfer, the concentration flux is also generated by temperature gradient (2006); this phenomenon is known as the Soret effect. The Soret effect can be neglected for the problems in which the concentration level of the diffusing species is very low, but this effect is significant as most of the heat and mass transport processes are governed by the simultaneous influence of buoyancy force due to mass and thermal diffusion. These transport processes are detected in combustion systems, nuclear reactor safety, furnace design, glass production, etc. Postelnicu (2004) has studied the effect of a magnetic field on heat and mass transfer by natural convection from vertical surfaces in porous media considering Soret and Dufour effects.

Influenced by above literature, we (2017) extended our previous work to study the effects of Soret number, Hall and ion slip parameters on MHD flow near the oscillatory infinite flat plate in a rotating system through porous medium. The governing partial differential equations of the

model have been solved analytically by using the Laplace transform method. The effect of various parameters, involved in the problem, on velocity, temperature and concentration are presented and discussed graphically.

2. Mathematical Formulation and Solution of the Model

Consider an unsteady flow of an incompressible, viscous and electrically conducting fluid near oscillatory vertical infinite plate in a porous medium. Let the direction of oscillation is along the *x*- axis, and *z*- axis is chosen normal to the plate. Consider *y* - axis perpendicular to the *x*-*z* plane. The plate is assumed to coincide with plane *z* = 0. Also, the system is rotating with a constant angular velocity Ω about *z* - axis. The plate under consideration is taken to be electrically non-conducting and let a magnetic field of uniform strength B_o is imposed along *z*- axis. As the plate occupying the plane *z* = 0 is of infinite extent, all the physical quantities depend only on *z* and *t*.

Initially, at time $t \le 0$, the fluid and the plate are at rest and at a uniform concentration C_∞ and temperature T_∞. At time $t > 0$, the plate starts to oscillate with a velocity $u_o Sin\omega t$ in its own plane; and the temperature and concentration of the plate is raised to T_s and C_s respectively. Since the fluid is electrically conducting whose magnetic Reynolds number is very small, hence the induced magnetic field produced by the fluid motion is negligible in comparison to the applied one. Also, due to the conservation of electric charge, current density along *z*- direction j_z is constant. Since the plate is assumed to be non-conducting, j_z can be taken as zero. So, under the above assumptions, the governing equations with Boussinesq's approximation are as follows:

$$\frac{\partial u}{\partial t} - 2\Omega v = \upsilon \frac{\partial^2 u}{\partial z^2} + g\beta(T - T_\infty) + g\beta^*(C - C_\infty) + \frac{B_o}{\rho} j_y - \frac{\upsilon}{K} u, \tag{1}$$

$$\frac{\partial v}{\partial t} + 2\Omega u = \upsilon \frac{\partial^2 v}{\partial z^2} - \frac{B_o}{\rho} j_x - \frac{\upsilon}{K} v, \tag{2}$$

$$\frac{\partial C}{\partial t} = D \frac{\partial^2 C}{\partial z^2} + \frac{D_T k_T}{T_m} \frac{\partial^2 T}{\partial z^2}, \tag{3}$$

$$\frac{\partial T}{\partial t} = \alpha \frac{\partial^2 T}{\partial z^2}, \tag{4}$$

where

$$j_x = \frac{\sigma B_o \{(1 + m\, m_i)v + m\, u\}}{(1 + m\, m_i)^2 + m^2}, \quad j_y = \frac{\sigma B_o \{m\, v - (1 + m\, m_i)u\}}{(1 + m\, m_i)^2 + m^2}.$$

The boundary conditions taken are as under:

$$\left.\begin{aligned} &t \le 0 : u(z,\ t) = 0,\ v(z,\ t) = 0,\ C(z,\ t) = C_\infty,\ T(z,\ t) = T_\infty \\ &t > 0 : u(0,\ t) = u_o \operatorname{Sin} \omega t,\ v(0,\ t) = 0,\ T(0,\ t) = T_s \left(> T_\infty\right),\ C(0,\ t) = C_s \left(> C_\infty\right) \\ &as\ z \to \infty; (z,\ t) \to 0,\ v(z,\ t) \to 0,\ C(z,\ t) \to C_\infty,\ T(z,\ t) \to T_\infty. \end{aligned}\right\} \tag{5}$$

To obtain the equations in dimensionless form, the following non-dimensional quantities are introduced:

$$\left.\begin{aligned} &u' = \frac{u}{u_o},\ v' = \frac{v}{u_o},\ t' = \frac{u_o^2}{\upsilon} t,\ z' = \frac{u_o}{\upsilon} z,\ \theta = \frac{(T - T_\infty)}{(T_s - T_\infty)},\ \phi = \frac{(C - C_\infty)}{(C_s - C_\infty)}, \\ &G_m = \frac{g \beta^* \upsilon (C_s - C_\infty)}{u_o^3},\ S_c = \frac{\upsilon}{D},\ \mathrm{P}_r = \frac{\upsilon}{\alpha},\ \mathrm{S}_r = \frac{D_T k_T (T_s - T_\infty)}{T_m \upsilon (C_s - C_\infty)}, \\ &M = \frac{\sigma B_o^2 \upsilon}{\rho u_o^2},\ G_r = \frac{g \beta \upsilon (T_s - T_\infty)}{u_o^3},\ \Omega' = \frac{\upsilon}{u_o^2} \Omega,\ \omega' = \frac{\upsilon}{u_o^2} \omega,\ K' = \frac{u_o^2}{\upsilon^2} K. \end{aligned}\right\} \tag{6}$$

By using (6), the equations (1), (2), (3), (4) and (5) become:

$$\frac{\partial u'}{\partial t'} - 2\Omega' v' = \frac{\partial^2 u'}{\partial z'^2} + \frac{M}{(1 + m\ m_i)^2 + m^2} \{m\ v' - (1 + m\ m_i) u'\} + G_m \phi + G_r \theta - \frac{u'}{K'}, \tag{7}$$

$$\frac{\partial v'}{\partial t'} + 2\Omega' u' = \frac{\partial^2 v'}{\partial z'^2} - \frac{M}{(1 + m\ m_i)^2 + m^2} \{(1 + m\ m_i) v' + m\ u'\} - \frac{v'}{K'}, \tag{8}$$

$$\frac{\partial \phi}{\partial t'} = \frac{1}{S_c} \frac{\partial^2 \phi}{\partial z'^2} + S_r \frac{\partial^2 \theta}{\partial z'^2}, \tag{9}$$

$$\frac{\partial \theta}{\partial t'} = \frac{1}{P_r} \frac{\partial^2 \theta}{\partial z'^2}, \tag{10}$$

$$\left.\begin{aligned} &t' \le 0 : u'(z',\ t') = 0,\ v'(z',\ t') = 0,\ \phi(z',\ t') = 0,\ \theta(z',\ t') = 0 \\ &t' > 0 : u'(0,\ t') = Sin(\omega' t'),\ v'(0,\ t') = 0,\ \phi(0,\ t') = 1,\ \theta(0,\ t') = 1 \\ &as\ z' \to \infty;\ u'(z',\ t') \to 0,\ v'(z',\ t') \to 0,\ \phi(z',\ t') \to 0,\ \theta(z',\ t') \to 0. \end{aligned}\right\} \tag{11}$$

After removing the primes ('), the equations (7) to (11) are rewritten as

$$\frac{\partial u}{\partial t} - 2\Omega v = \frac{\partial^2 u}{\partial z^2} + \frac{M}{(1 + m\ m_i)^2 + m^2} \{m\ v - (1 + m\ m_i) u\} + G_m \phi + G_r \theta - \frac{u}{K}, \tag{12}$$

$$\frac{\partial v}{\partial t} + 2\Omega u = \frac{\partial^2 v}{\partial z^2} - \frac{M}{(1 + m\ m_i)^2 + m^2} \{(1 + m\ m_i) v + m\ u\} - \frac{v}{K}, \tag{13}$$

$$\frac{\partial \phi}{\partial t} = \frac{1}{S_c} \frac{\partial^2 \phi}{\partial z^2} + S_r \frac{\partial^2 \theta}{\partial z^2}, \tag{14}$$

$$\frac{\partial \theta}{\partial t} = \frac{1}{P_r} \frac{\partial^2 \theta}{\partial z^2}, \tag{15}$$

.

$$\left.\begin{array}{l} t \le 0 : u(z,\ t) = 0,\ v(z,\ t) = 0,\ \phi(z,\ t) = 0,\ \theta(z,\ t) = 0 \\ t > 0 : u(0,\ t) = Sin(\omega t),\ v(0,\ t) = 0,\ \phi(0,\ t) = 1,\ \theta(0,\ t) = 1 \\ as\ z \to \infty;\ u(z,\ t) \to 0,\ v(z,\ t) \to 0,\ \phi(z,\ t) \to 0,\ \theta(z,\ t) \to 0. \end{array}\right\} \tag{16}$$

To solve above system, take $V = u + iv,$ on combining equation (12) and (13), we get,

$$\frac{\partial V}{\partial t} = \frac{\partial^2 V}{\partial z^2} - bV + G_m\phi + G_r\theta, \tag{17}$$

The boundary conditions (16) are reduced to:

$$\left.\begin{array}{l} t \le 0 : V(z,\ t) = 0,\ \phi(z,\ t) = 0,\ \theta(z,\ t) = 0 \\ t > 0 : V(0,\ t) = Sin(\omega t),\ \phi(z,t) = 1,\ \theta(z,t) = 1 \\ as\ z \to \infty; V(z,\ t) \to 0,\ \phi(z,\ t) \to 0,\ \theta(z,\ t) \to 0. \end{array}\right\} \tag{18}$$

The governing non-dimensional partial differential equations (14), (15) and (17) subjects to boundary conditions (18) are solved using the Laplace Transform technique. The solution is as under:

$$\begin{aligned} V(z,\ t) = {} & \frac{i}{2}\left\{e^{-i\omega t}Cosh(a_1 z) - e^{i\omega t}Cosh(a_2 z)\right\} - \frac{ie^{-i\omega t}}{4}\left\{e^{-a_1 z}Erf\left(\eta - a_1\sqrt{t}\right) + e^{a_1 z}Erf\left(\eta + a_1\sqrt{t}\right)\right\} \\ & + \frac{ie^{i\omega t}}{4}\left\{e^{-a_2 z}Erf\left(\eta - a_2\sqrt{t}\right) + e^{a_2 z}Erf\left(\eta + a_2\sqrt{t}\right)\right\} + \alpha_3 e^{-B_2 t}\left\{e^{-a_5 z}Erfc\left(\eta - a_5\sqrt{t}\right) + e^{a_5 z}Erfc\left(\eta + a_5\sqrt{t}\right)\right\} \\ & + 2\alpha_2 Erfc(a_8\eta) - \alpha_2 e^{-B_1 t}\left\{2Cosh(a_6 z) + e^{-a_6 z}Erf\left(a_7\sqrt{t} - a_8\eta\right) - e^{a_6 z}Erfc\left(a_7\sqrt{t} + a_8\eta\right)\right\} \\ & - \alpha_3 e^{-B_2 t}\left\{2Cosh(a_9 z) + e^{-a_9 z}Erf\left(a_{10}\sqrt{t} - a_{11}\eta\right) - e^{a_9 z}Erfc\left(a_{10}\sqrt{t} + a_{11}\eta\right)\right\} + 2\alpha_3 Erfc(a_{11}\eta) \\ & + \alpha_1\left\{2Cosh(a_3 z) + e^{-a_3 z}Erf\left(a_3\sqrt{t} - \eta\right) - e^{a_3 z}Erf\left(a_3\sqrt{t} + \eta\right)\right\} \\ & + \alpha_2 e^{-B_1 t}\left\{e^{-a_4 z}Erfc\left(\eta - a_4\sqrt{t}\right) + e^{a_3 z}Erfc\left(\eta + a_4\sqrt{t}\right)\right\} \end{aligned}$$

$$\theta(z,\ t) = Erfc(a_8 z)$$

$$\phi(z,\ t) = (1+a)Erfc(a_{11}\eta) - a\ Erfc(a_8 z)$$

3. Skin Friction, Nusselt number and Sherwood number

The shear stress components in the primary and secondary directions are given by the following expressions:

$$\tau_x(z,\ t) = -\mu\frac{\partial u}{\partial z},\quad \tau_y(z,\ t) = -\mu\frac{\partial v}{\partial z}.$$

By using non- dimensional variables given in (6), the dimensionless stresses are as follows:

$$\tau_1(z', t') = \frac{\tau_x}{\rho u_o^2},\ \tau_2(z', t') = \frac{\tau_y}{\rho u_o^2}.$$

And by using the complex notation, we get

$$\tau(z', t') = \tau_1(z', t') + i\tau_2(z', t').$$

After removing the prime ($'$), the dimensionless shear stress can be written as:

$$\tau(z, t) = \tau_1(z, t) + i\tau_2(z, t) = -\frac{\partial V(z, t)}{\partial z}.$$

Hence, the non-dimensional skin friction coefficient at the plate in complex form is given by

$$S_f(t) = \tau(0, t) = \frac{i}{4}e^{-i\omega t}\left\{\frac{2e^{-a_1^2 t}}{\sqrt{\pi t}} + 2a_1 Erf\left(a_1\sqrt{t}\right)\right\} - \frac{i}{4}e^{i\omega t}\left\{\frac{2e^{-a_2^2 t}}{\sqrt{\pi t}} + 2a_2 Erf\left(a_2\sqrt{t}\right)\right\}$$
$$+\alpha_1\left\{\frac{2e^{-a_3^2 t}}{\sqrt{\pi t}} + 2a_3 Erf\left(a_3\sqrt{t}\right)\right\} + \alpha_2 e^{-B_1 t}\left\{\frac{2e^{-a_4^2 t}}{\sqrt{\pi t}} + a_4 Erfc\left(-a_4\sqrt{t}\right) - a_4 Erfc\left(a_4\sqrt{t}\right)\right\}$$
$$-\alpha_2 e^{-B_1 t}\left\{\frac{2a_8 e^{-a_7^2 t}}{\sqrt{\pi t}} + 2a_6 Erf\left(a_7\sqrt{t}\right)\right\} - \alpha_3 e^{-B_2 t}\left\{\frac{2a_{11} e^{-a_{10}^2 t}}{\sqrt{\pi t}} + 2a_9 Erf\left(a_{10}\sqrt{t}\right)\right\}$$
$$+\frac{2(\alpha_2 a_8 + \alpha_3 a_{11})}{\sqrt{\pi t}} + \alpha_3 e^{-B_2 t}\left\{\frac{2e^{-a_5^2 t}}{\sqrt{\pi t}} + a_5 Erfc\left(-a_5\sqrt{t}\right) - a_5 Erfc\left(a_5\sqrt{t}\right)\right\}$$

The dimensionless skin friction coefficients in the primary and secondary direction respectively are obtained as:

$$S_{f_x} = Re(S_f),\ S_{f_y} = Im(S_f).$$

Again, by using the dimensionless variables given in (6), the expressions for non-dimensional Nusselt number and Sherwood number, respectively, may be given as:

$$Nu = \frac{a_8}{\sqrt{\pi t}},\ Sh = \frac{(1+a)a_{11} - aa_8}{\sqrt{\pi t}}.$$

4. Result and Discussion

Figures 1 to 13 show the effects of various physical parameters on velocity, temperature and concentration distribution near the plate at a particular instant of time. From the figures 1 to 8 it

is observed that the velocity components, along the direction of motion of the plate (primary velocity *u*), and along the transverse direction (secondary velocity *v*), have different maximum values near the plate ($z < 1$). Figures 1 to 4 depict the influence of Soret number. It is observed that an increase in the Soret number corresponds to an increase in both components of the velocity, hence increasing the momentum boundary layer thickness. The effect of rotation parameter is shown in figure 5; it can be seen that the primary velocity decreases and the secondary velocity increases with an increase in the rotation parameter. Also, it is noticed that the effect of rotation parameter is significant for secondary velocity as compared with primary velocity (figures 1, 2 and 5).

Effect of the ion-slip parameter on the fluid velocity is depicted in figures 6 and 7 for different values of magnetic field. It is found that when m_i is increased the primary velocity increases and secondary velocity decreases with constant rotation. This is due to the fact that an increase in m_i reduces the magnetic force on *u*. It is also noticed that these variations in both the components of velocities with m_i are considerable only when the strength of applied magnetic field is strong. Figure 8 shows how the velocity varies with Hall parameter. Here it can be seen that the variation is similar to that of ion slip parameter. Figures 9, 10 and 11 display the concentration profiles near the plate. Variation in the concentration with Schmidt number is shown in figure 9. Here it shows that the concentration in the system decreases with the increase in Schmidt number. Similar behavior on temperature profile is shown by Prandtl number (figure 13). From figure 11, it is observed that an increase in the Soret number corresponds to an increase in the concentration. Figures 10 and 12 show the relationship of temperature and concentration with time.

Sherwood number and Nusselt number are plotted against time in figures 14 to 16. Here it is observed that initially these numbers achieved a maximum value at the plate, and then decrease continuously as the time increases. From figure 14 it is found that Sherwood number decreases with increase in Soret number. Also, Sherwood number is decreased with increase in the Schmidt number (figure-15). A similar effect is observed for Nusselt number with Prandtl number (figure16).

Further, the variation in the skin-friction coefficient at a particular instant of time ($t = 0.4$), with various physical parameters, is shown in tables 1 to 4. It is seen from the table-2 that the skin-friction components along the primary and secondary directions go on decreasing with increase in the Soret number as well as porosity of the medium. The skin-friction coefficient along primary direction (S_{f_x}) decreases with the increase in Hall parameter, and it is increased with increase in magnetic field parameter (table-1). Table-1 also shows that these parameters exhibit reverse effect on S_{f_y}. Table-3 displays the effect of ion-slip parameter on the skin friction coefficients. Changes in skin-friction coefficients with the oscillation frequency of the plate and rotation can be seen from the table-4.

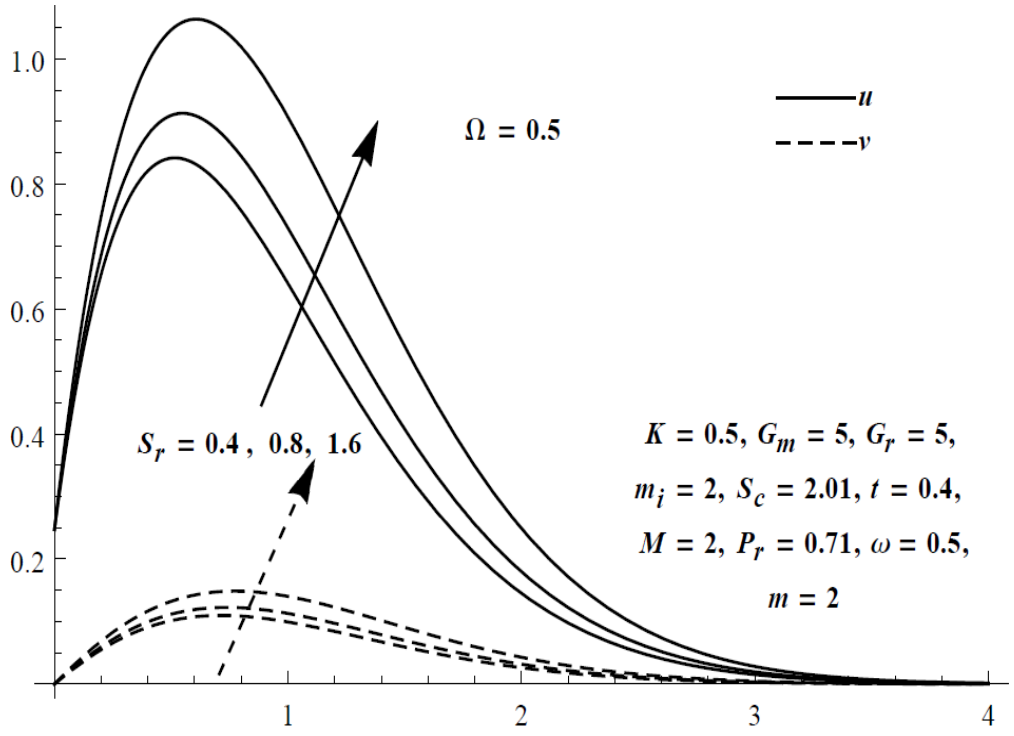

Figure 1. Velocity profile for S_r at $\Omega = 0.5$

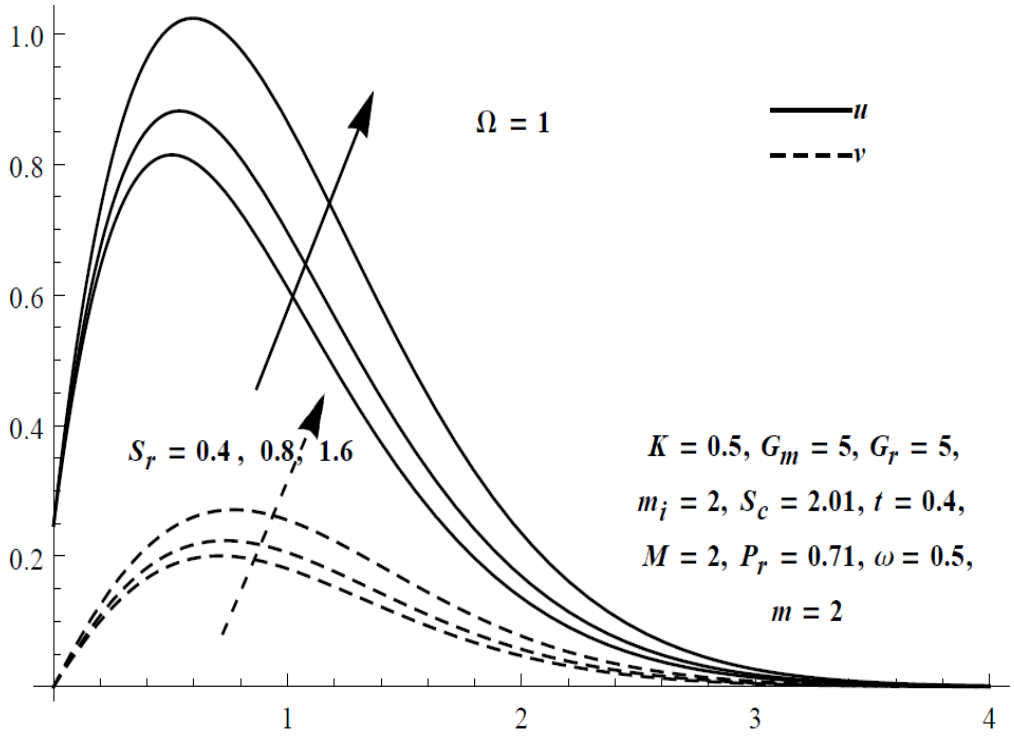

Figure 2. Velocity profile for S_r at $\Omega = 1$

.

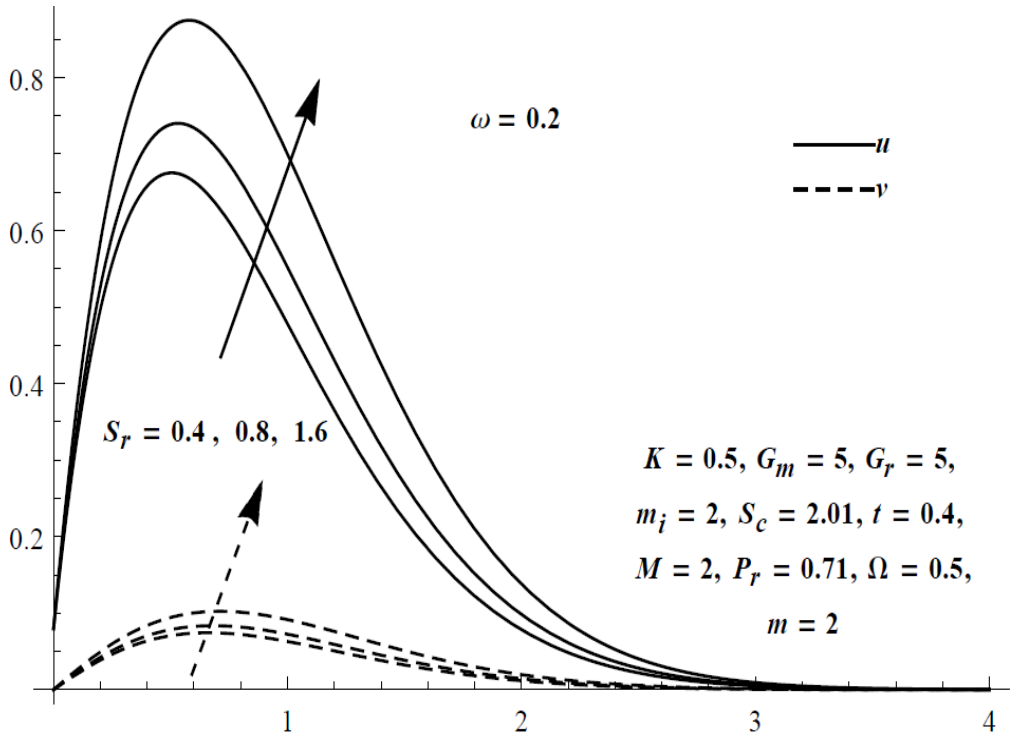

Figure 3. Velocity profile for S_r at $\omega = 0.2$

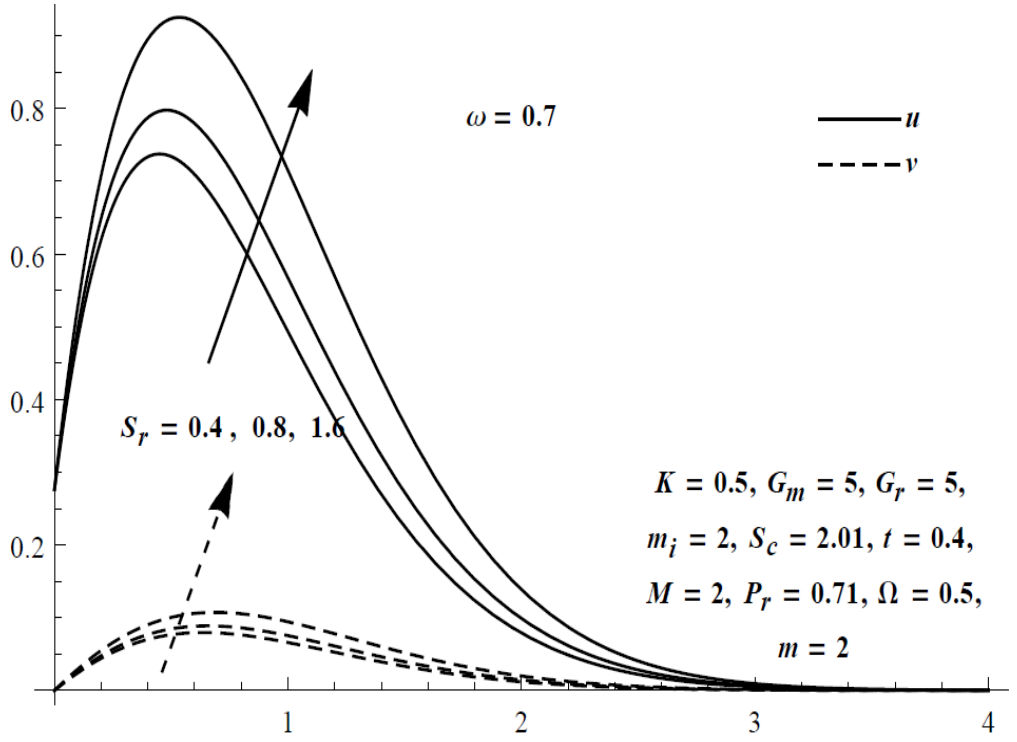

Figure 4. Velocity profile for S_r at $\omega = 0.7$

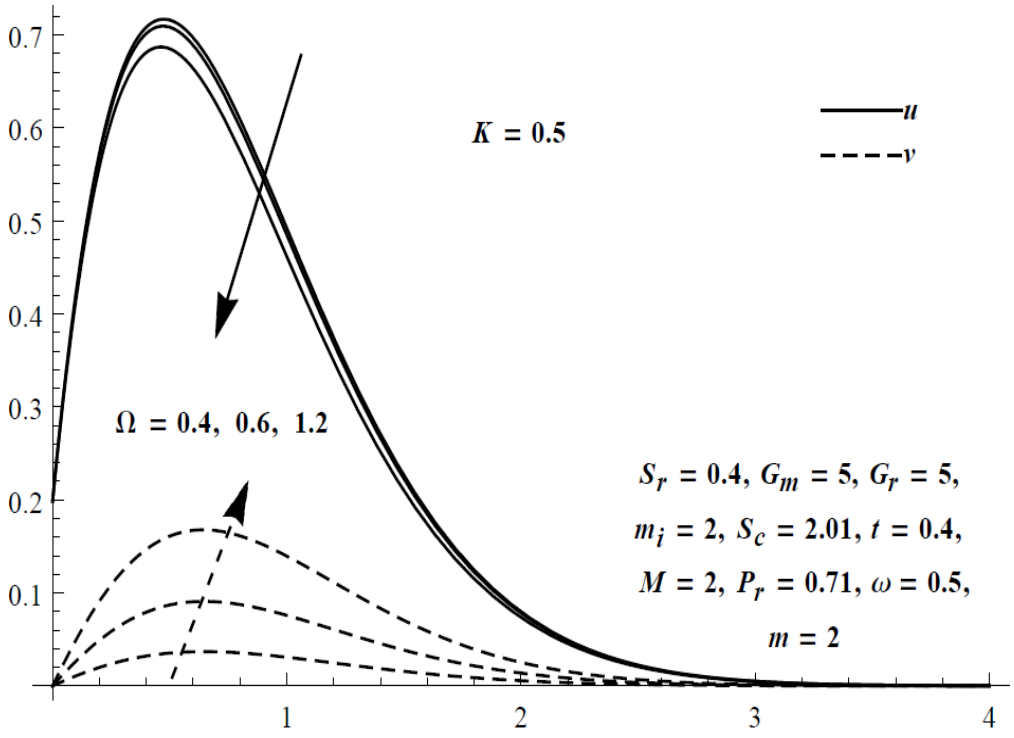

Figure 5. Velocity profile for Ω at $K = 0.5$

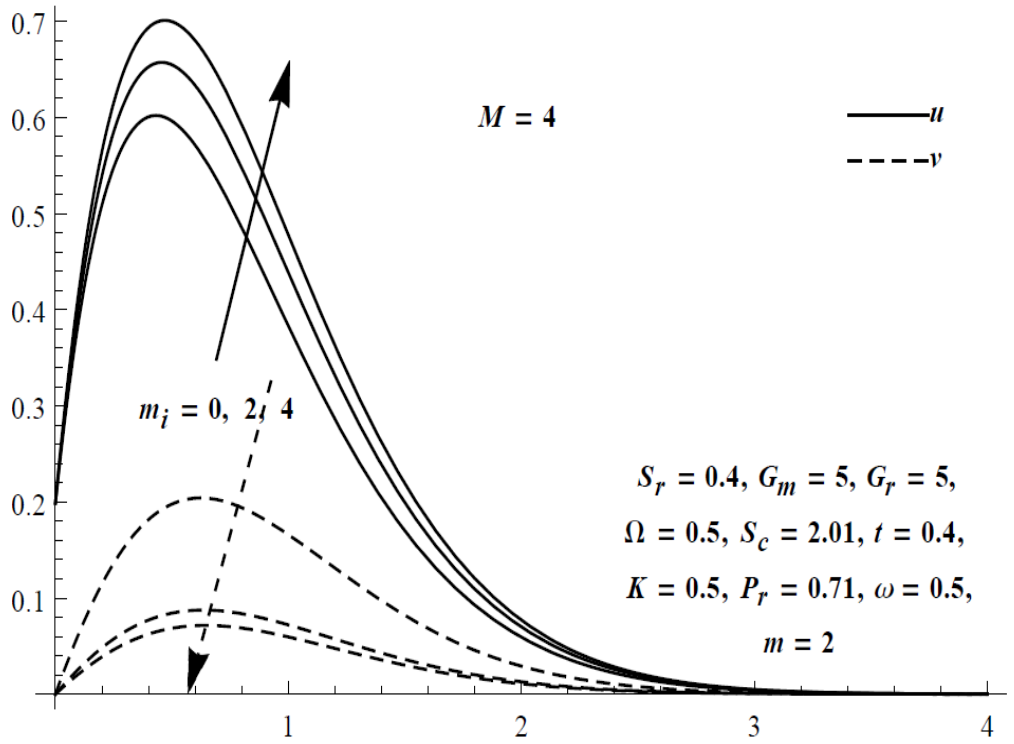

Figure 6. Velocity profile for m_i at $M = 4$

.

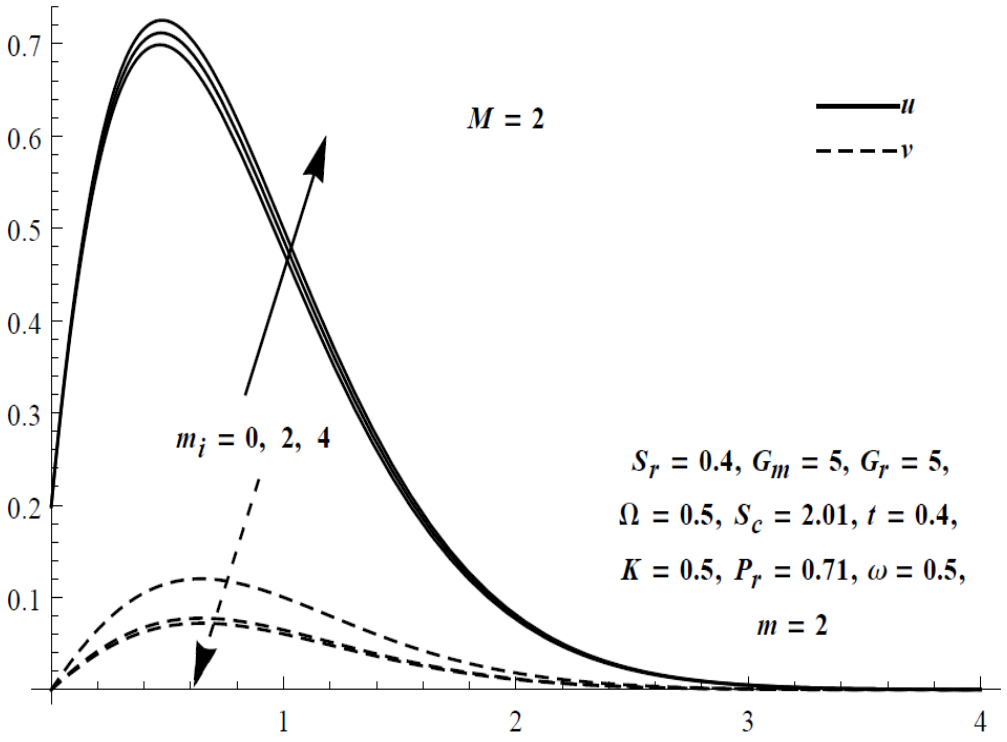

Figure 7. Velocity profile for m_i at $M = 2$

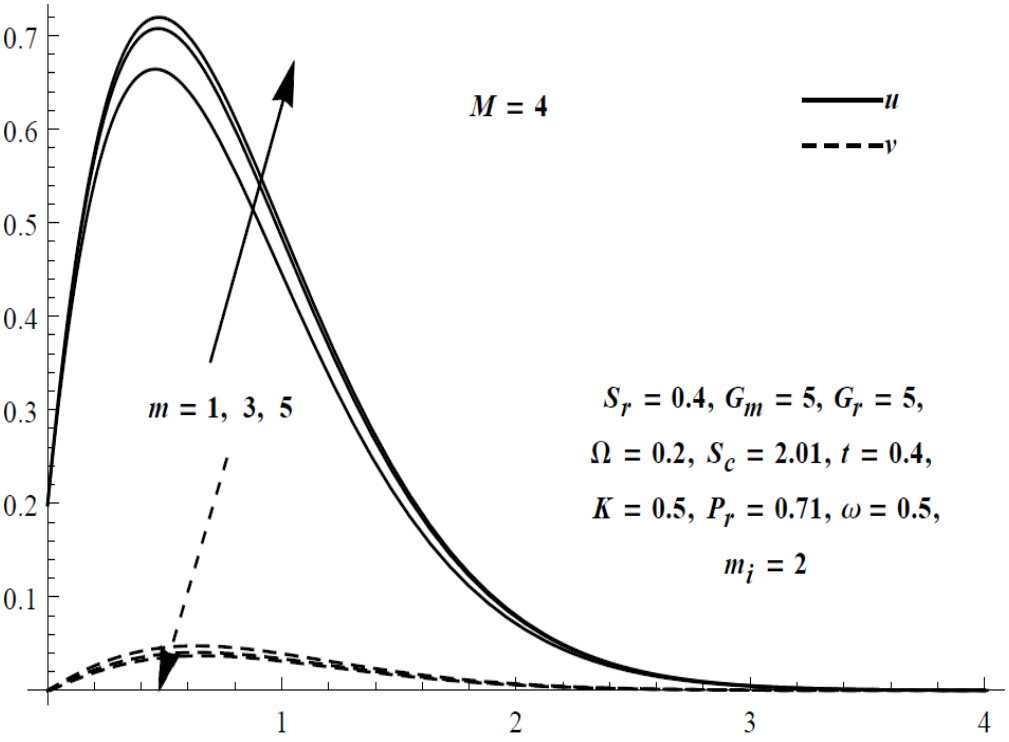

Figure 8. Velocity profile for m at $M = 4$

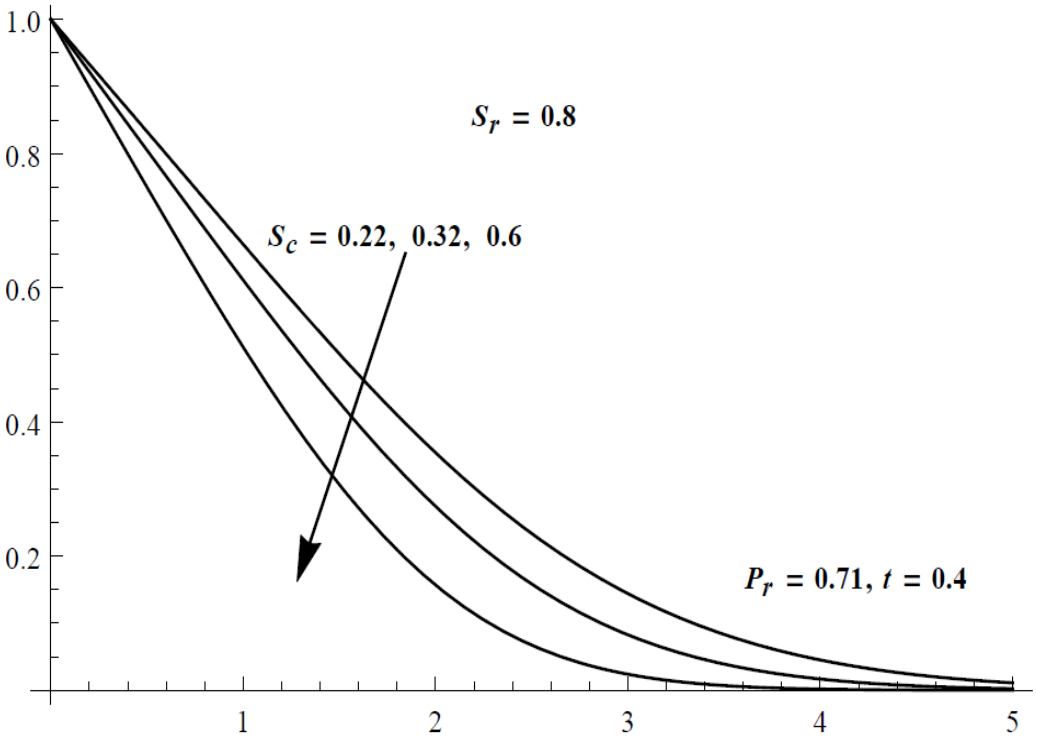

Figure 9. Concentration profile for S_c at $S_r = 0.8$

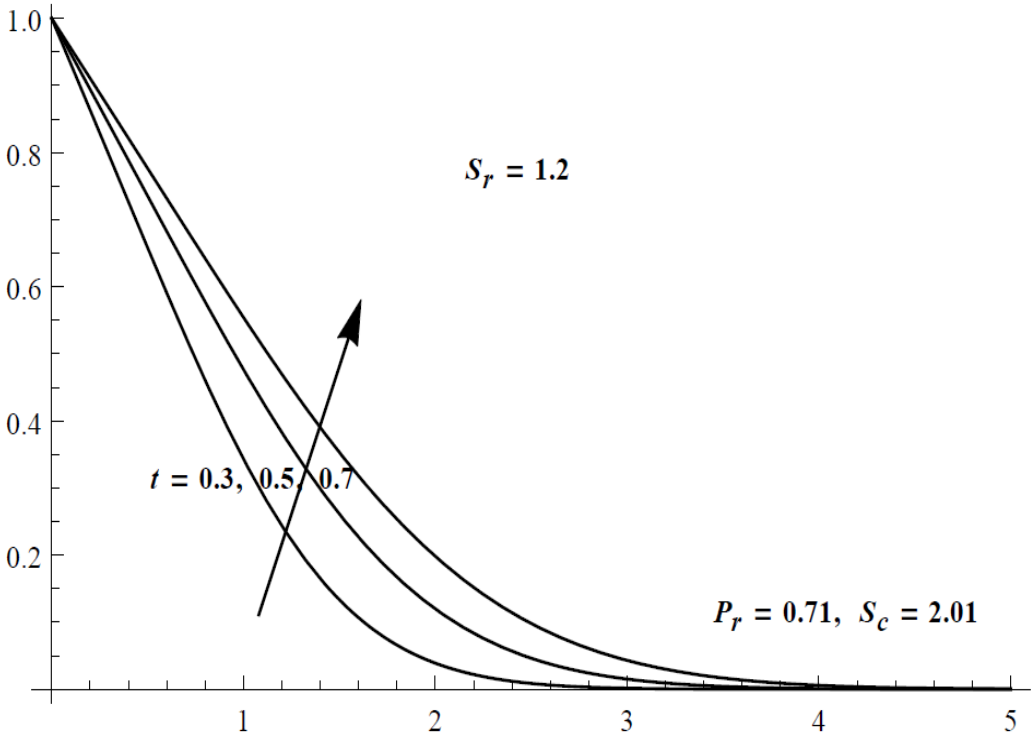

Figure 10. Concentration profile for time at $S_r = 1.2$

.

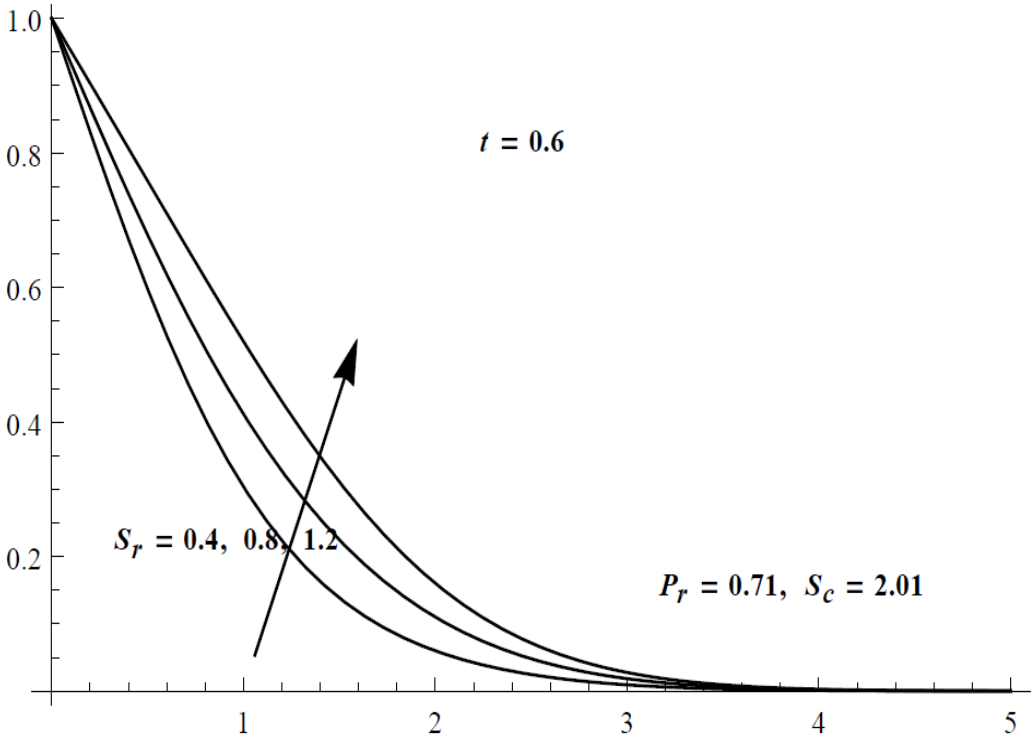

Figure 11. Concentration profile for S_r at $t = 0.6$

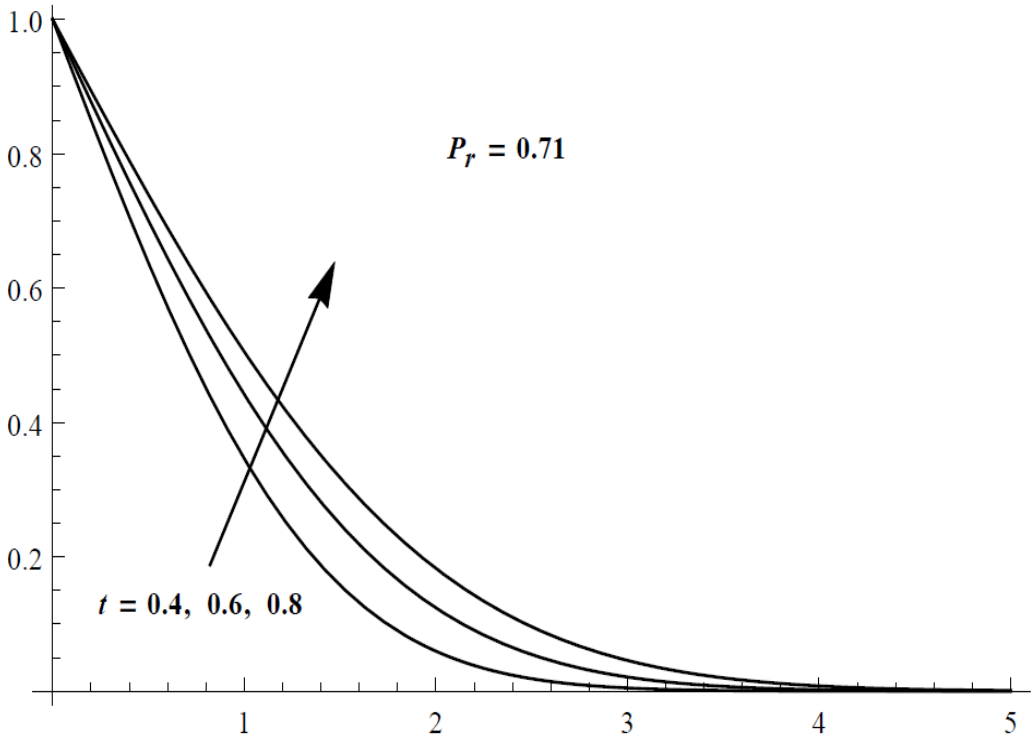

Figure 12. Temperature profile for time

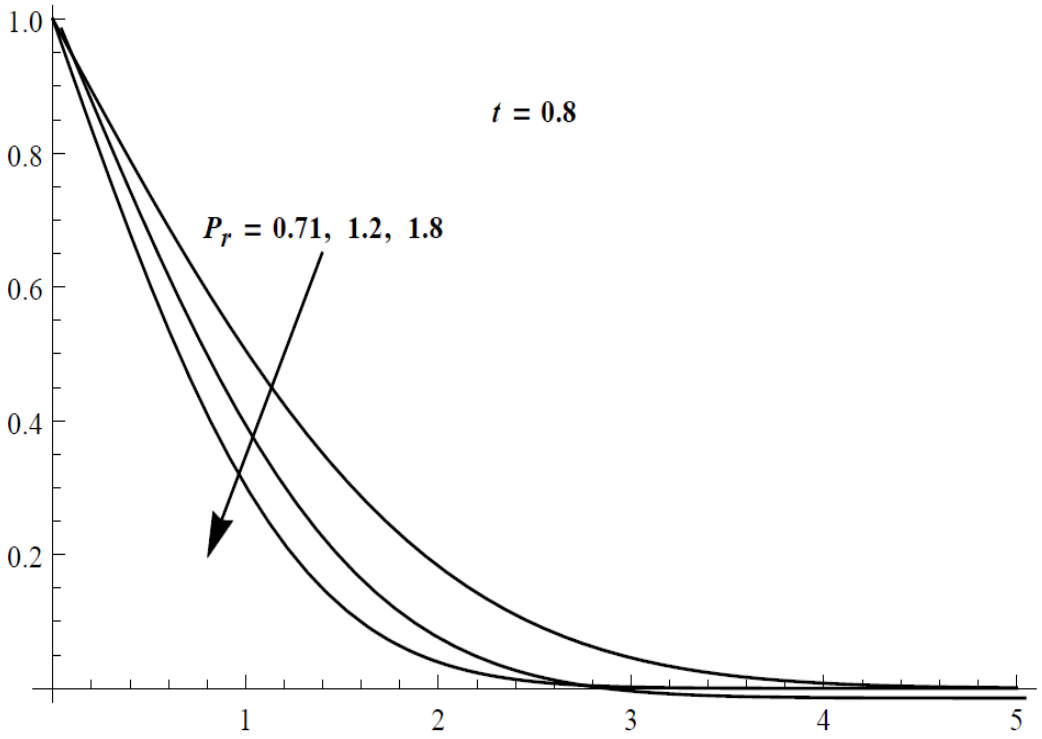

Figure 13. Temperature profile for P_r

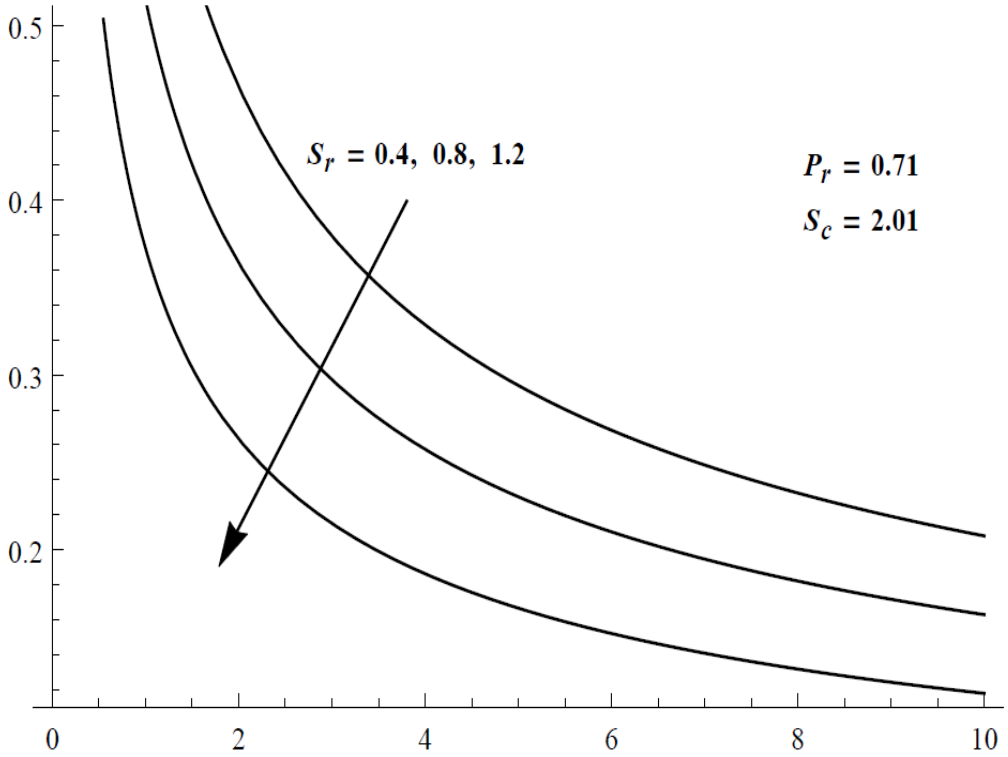

Figure 14. Sherwood number profile for S_r against time

.

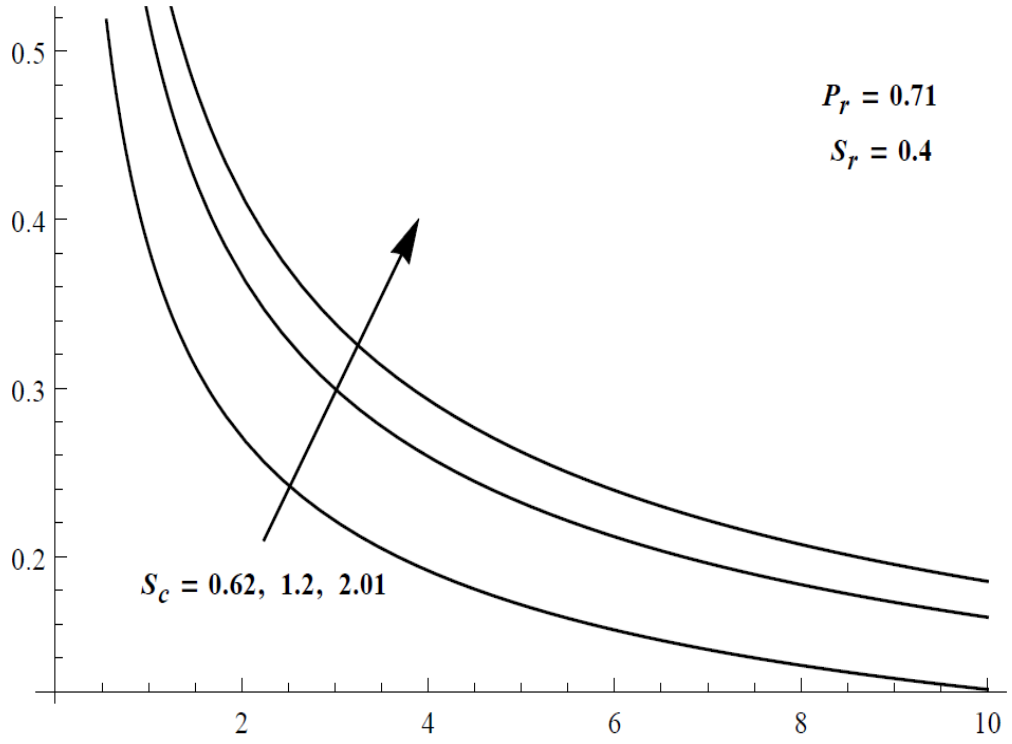

Figure 15. Sherwood number profile for S_c against time

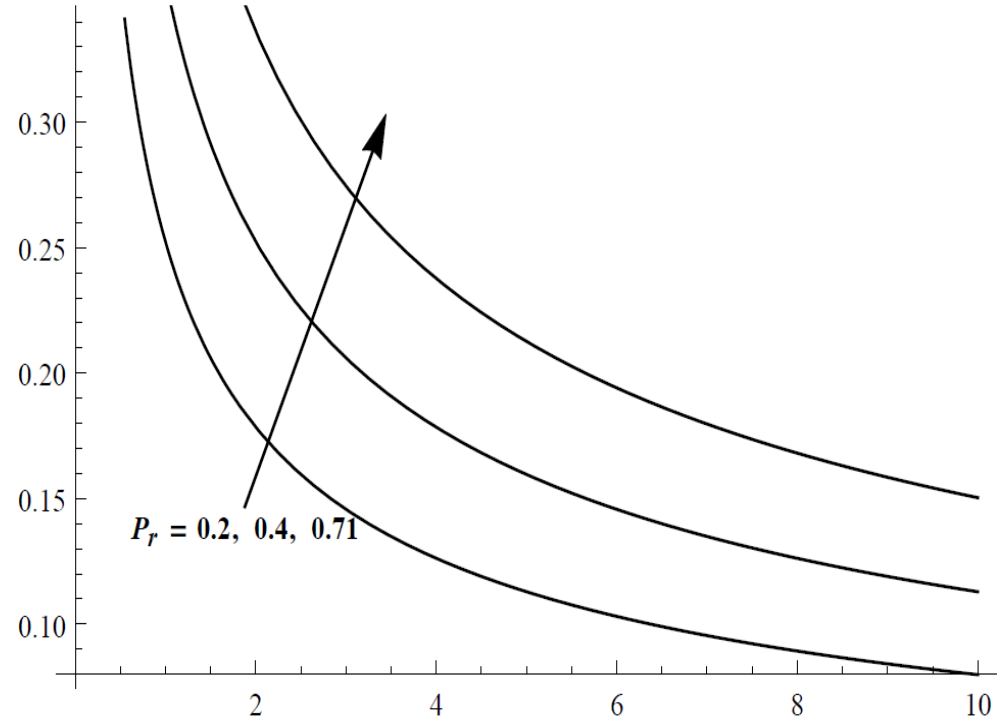

Figure 16. Nusselt number profile for P_r against time

Table 1.

Skin Friction for Hall parameter
$S_r = 0.4, K = 0.5, m_i = 2, \omega = 0.5, \Omega = 0.2,$
$S_c = 2.01, P_r = 0.71, G_r = 5, G_m = 5.$

m	$M = 2$		$M = 4$	
	$-S_{f_x}$	$-S_{f_y}$	$-S_{f_x}$	$-S_{f_y}$
1	2.6163	0.1234	2.4945	0.1526
3	2.6930	0.1084	2.6404	0.1267
5	2.7131	0.1021	2.6797	0.1148

Table 2.

Skin Friction for Soret number
$M = 2, m = 2, m_i = 2, \omega = 0.5, \Omega = 0.2,$
$S_c = 2.01, P_r = 0.71, G_r = 5, G_m = 5.$

S_r	$K = 0.5$		$K = 5.0$	
	$-S_{f_x}$	$-S_{f_y}$	$-S_{f_x}$	$-S_{f_y}$
0.4	2.6704	0.1143	3.0957	0.1456
0.8	2.8234	0.1233	3.2835	0.1580
1.2	2.9764	0.1322	3.4713	0.1704

Table 3.

Skin Friction for Ion-Slip parameter
$K = 0.5, m = 2, \omega = 0.5, M = 2, S_r = 0.4,$
$S_c = 2.01, P_r = 0.71, G_r = 5, G_m = 5.$

m_i	$\Omega = 0.1$		$\Omega = 1.0$	
	$-S_{f_x}$	$-S_{f_y}$	$-S_{f_x}$	$-S_{f_y}$
0	2.6492	0.2104	2.5598	0.5727
2	2.6728	0.0719	2.6130	0.4463
4	2.7020	0.0535	2.6451	0.4353

Table 4.

Skin Friction for Oscillation frequency
$K = 0.5, m = 2, m_i = 2, M = 2, S_r = 0.4,$
$S_c = 2.01, P_r = 0.71, G_r = 5, G_m = 5.$

ω	$\Omega = 0.1$		$\Omega = 1.0$	
	$-S_{f_x}$	$-S_{f_y}$	$-S_{f_x}$	$-S_{f_y}$
0.2	2.9443	0.0638	2.8880	0.3955
0.4	2.7625	0.0692	2.7039	0.4295
0.6	2.5840	0.0745	2.5231	0.4631

5. Conclusion

An analytical study has been done for the model under consideration by converting the governing linear partial differential equations into non-dimensional form. It is found that, at a particular instant of time (t = 0.4), the extreme values of the components of the velocity along the primary direction and transverse direction appear in interval $0.4 \le z \le 1$. Also, the maximum values of the concentration and temperature occur at the plate. The velocity in both the directions can be increased by increasing the Soret number. When the Hall or Ion-Slip parameters are

increased, the velocity in the primary direction increases whereas the secondary component of the velocity is decreased. Rotation retards the primary flow and accelerates the secondary flow. It is also observed that the concentration in the system decreases with the increase in the Schmidt number; whereas it increases with the increase in the Soret number. Further, an increase in the Prandtl number can reduce the temperature in the system. The model under consideration can be expanded into studies of flow past spheres, cylinders, cones, and wedges etc, according to the required applications.

Acknowledgement

Our sincere thanks to the honorable Editor-in-Chief, Professor Aliakbar M. Haghighi; the reviewers; each member of the Editorial Board; and the staff of the Journal 'Application and applied Mathematics' for their valuable comments and suggestions which helped in improving the manuscript.

REFRENCES

Abo-Eldahab, E.M. and Elbarbary, E.M.E. (2001). Hall current effect on magnetohydrodynamic free-convection flow past a semi-infinite vertical plate with mass transfer, Int. J. Engg. Sci.39: 1641-1652.

Agarwal, H.L., Ram, P.C. and Singh, V (1983). Combined influence of dissipation and Hall effect on free convective in a rotating fluid, .Indian J. Pure appl. Math. 14(3):314-32.

Attia, H.A. (2005). Unsteady couette flow with heat transfer considering ion-slip, Turk J Phys 29, 379 - 388.

Attia, H.A.(2009). Ion slip effect on unsteady couette flow with heat transfer under exponential decaying pressure gradient, Tamkang Journal of Science and Engineering, Vol. 12, No. 2, pp. 209-214.

Cowling, T.G. (1957). *Magneto hydrodynamics*, New York, Interscience Publishers.

Ganesan, P. and Laganathan, P. (2002). Radiation and Mass transfer effects on flow of an incompressible viscous fluid past a moving cylinder, Int. J.of Heat and Mass Transfer, vol. 45, pp. 4281-4288.

Greenspan, H. P. (1968). *The Theory of Rotating Fluids*, Cambridge University Press, London.

Hossain, M.A. and Takhar, H.S. (1996). Radiation effect on mixed convection along a vertical plate with uniform surface temperature, Heat Mass Transfer 31, 243–248.

Jaimala, Vikrant and Kumar Vivek. (2013). Thermal Convection in a Couple-Stress Fluid in the Presence of Horizontal Magnetic Field with Hall Currents. Application and applied Mathematics, Vol.8, Issue 1, pp. 161-117.

Mazumdar, B.S.,Gupta, A.S. and Datta, N.(1976). Flow and heat transfer in hydrodynamic ekman layer on a porous plate with Hall effects, Int.J.heat mass Transfer,19,523.

Muthucumaraswamy, R. Ganesan, P. and Soundalgeker, V.M. (2001). Heat and mass transfer effect on flow past impulsively started vertical plate, Acta Mechanica ,Vol 146 (1), pp1-8.

Muthucumaraswamy, R., Dhanasekar, N. and Prasad, G. E. (2013). Rotation effects onunsteady flow past an accelerated isothermal vertical plate with variable mass transfer in the presence of chemical reaction of first order, J. Appl. Fluid Mech. 6 (4), 485 – 490.

Owen, J. M. and Rogers, R. H. (1989). Flow and heat transfer in rotating disc systems, Vol . I, Rotor – Stator Systems, John Wiley Sons, New York.

Platten, J.K. (2006). The Soret effect: A review of recent experimental results, Journal of applied mechanics Vol 73, 5-15.

Postelnicu, A. (2004). Influence of a magnetic field on heat and mass transfer by natural convection from vertical surfaces in porous media considering Soret and Dufour effects. Int. J. H & M Transfer, 47, 1467-1475.

Prasad, V.R., Bhaskar Reddy, N. and Muthucumaraswamy, R. (2007). Radiation and mass transfer effects on two-dimensional flow past an impulsively started infinite vertical plate, International Journal of Thermal Sciences 46, 1251–1258.

Rajput, U.S. and Shareef, M. (2017). Unsteady MHD flow along exponentially accelerated vertical flat surface through porous medium with variable temperature and Hall current in a rotating system J Fundam Appl Sci., 9(2), 1050-1062.

Rajput, U.S. and Gaurav, K. (2016). Unsteady MHD flow past an impulsively started inclined plate with variable temperature and mass diffusion in the presence of Hall currents. Application and applied Mathematics, Vol.11, Issue 2, pp. 693-703.

Raptis, A. (1998). Radiation and free convection flow through a porous medium, Int. Comm. Heat Mass Transfer 25, 289–295.

Soong, C. Y. (2001). Thermal buoyancy effects in rotating non – isothermal flows, Int. J. Rotating Machinery Vol 7(6), 435 – 446.

Soong, C. Y. and Ma, H. L. (1995). Unsteady analysis of non – isothermal flow and heat transfer between rotating co-axial disks, Int. J. Heat Mass Transfer 38(10), 1865 – 1878.

Soundalgekar, V.M. (1979). Effects of Mass Transfer and Free-Convection Currents on the Flow Past an Impulsively Started Vertical Plate, J. Appl. Mech 46(4), 757-760.

Watanabe, T. and Pop, I. (1995). Hall effects on magnetohydrodynamic boundary layer flow over a continuous moving flat plate, Acta Mechanica. Vol 108 (1): pp35-47.

APPENDIX

$$b = \frac{Mi}{m + i(1 + mm_i)} + 2i\Omega + \frac{1}{K},$$

$$A_1 = \frac{G_r}{1 - P_r}, A_2 = \frac{G_m}{1 - S_c},$$

$$A_3 = \frac{G_m}{1 - P_r}, B_1 = \frac{b}{1 - P_r},$$

$$B_2 = \frac{b}{1 - S_c}, a = \frac{P_r S_c S_r}{P_r - S_c},$$

.

$$a_1=\sqrt{b-i\omega},a_2=\sqrt{b+i\omega},a_3=\sqrt{b},a_4=\sqrt{b-B_1},$$
$$a_5=\sqrt{b-B_2},a_6=\sqrt{-B_1P_r},a_7=\sqrt{-B_1},$$
$$a_8=\sqrt{P_r},a_9=\sqrt{-B_2S_c},$$
$$a_{10}=\sqrt{-B_2},a_{11}=\sqrt{S_c},\alpha_1=\frac{aA_3}{2B_1}-\frac{A_1}{2B_1}-\frac{(a+1)A_2}{2B_2},$$
$$\alpha_2=\frac{A_1-aA_3}{2B_1},\alpha_3=\frac{(a+1)A_2}{2B_2},\eta=\frac{z}{2\sqrt{t}}.$$

Nomenclature

D mass diffusion coefficient

G_m mass Grashof number

G_r thermal Grashof number

α thermal diffusivity

K permeability parameter

S_c Schmidt number

t' dimensionless time

k_T thermal diffusion ratio

u_0 amplitude of oscillatory velocity

v' dimensionless secondary velocity of the fluid

u primary velocity of the fluid

ω' dimensionless frequency of oscillation of the plate

β^* volumetric coefficient of concentration expansion

ν kinematic viscosity

μ dynamic viscosity

u' dimensionless primary velocity of the fluid

v secondary velocity of the fluid

g acceleration due to gravity

m_i Ion-slip parameter

M magnetic field parameter

P_r Prandtl number

S_r Soret number

ρ density of fluid

D_T thermal diffusion coefficient

K' dimensionless permeability parameter

ω frequency of oscillation of the plate

m Hall parameter

z' dimensionless spatial coordinate normal to the plate

β volumetric coefficient of thermal expansion

θ dimensionless temperature

ϕ dimensionless concentration

Ω' dimensionless rotation parameter

T_m mean fluid temperature